AIP Applied Physics Letters

Solar-blind AlGaN-based p-i-n photodetectors with high breakdown voltage and detectivity

Turgut Tut, Tolga Yelboga, Erkin Ulker, and Ekmel Ozbay

Citation: Appl. Phys. Lett. **92**, 103502 (2008); doi: 10.1063/1.2895643

View online: http://dx.doi.org/10.1063/1.2895643

View Table of Contents: http://apl.aip.org/resource/1/APPLAB/v92/i10

Published by the American Institute of Physics.

Solar-blind AlGaN-based *p-i-n* photodetectors with high breakdown voltage and detectivity

Turgut Tut,[a] Tolga Yelboga, Erkin Ulker, and Ekmel Ozbay
Nanotechnology Research Center, Department of Physics, and Department of Electrical and Electronics Engineering, Bilkent University, Bilkent, 06800 Ankara, Turkey

(Received 1 February 2008; accepted 12 February 2008; published online 10 March 2008)

We report on the high performance solar-blind AlGaN-based *p-i-n* photodetectors that are grown by metal-organic chemical vapor deposition on *c*-plane sapphire substrates. The dark current of the 200 μm diameter devices was measured to be on the order of 5 fA for bias voltages up to 10 V. The breakdown voltages were higher than 200 V. The responsivities of the photodetectors were 0.052 and 0.093 A/W at 280 nm under 0 and 40 V reverse biases, respectively. We achieved a detectivity of 7.5×10^{14} cm Hz$^{1/2}$/W for 200 μm diameter AlGaN *p-i-n* detectors. © *2008 American Institute of Physics*. [DOI: 10.1063/1.2895643]

The recent developments in high quality GaN/AlGaN material growth technology have led to the realization of high performance solar-/visible-blind photodetectors operating in the ultraviolet (UV) spectral region. Diverse applications wherein GaN/AlGaN-based photodetectors are utilized include engine/flame monitoring and detection, plant/vegetation growth monitoring, ozone layer monitoring, UV astronomy, gas detection, water purification, submarine communication, and medical applications.[1–5] These photodetectors are also chemically inert and suitable for harsh environments. GaN-based solid-state photodetectors with breakdown voltages ~100 V,[6–8] responsivities of 0.18 A/W at 360 nm (Ref. 9) (for Schottky-type photodetectors), and 0.2 A/W at 355 nm (for backilluminated GaN-based *p-i-n* photodetectors) that corresponds to 70% quantum efficiency (QE) at zero bias,[10] 3 dB bandwidth of 16 GHz [for metal-semiconductor-metal (MSM)-type photodetectors],[11] 2.6 GHz (for GaN-based Schottky-type photodetectors with indium tin oxide),[12] and 1.6 GHz (for *p-i-n*-type photodetectors)[13] have all been previously reported. AlGaN-based solar-blind photodetectors with breakdown voltages larger than 100 V, 136 mA/W responsivity under 0 V bias at 282 nm, and 72% QE under 5 V reverse bias for backilluminated AlGaN *p-i-n* photodiode,[14] solar-blind focal plane arrays that possess 60% QE at 280 nm under 0 V bias,[15] dark current density of 8.2×10^{-11} A/cm^2 under 5 V reverse bias,[16] and thermally limited detectivity of 4.9×10^{14} cm Hz$^{1/2}$/W (Ref. 17) at 267 nm have also been reported. In the present paper, we present our experimental results on high performance AlGaN-based solar-blind *p-i-n* photodetectors. Our solar-blind AlGaN photodetectors possess higher breakdown voltage, higher detectivity, and lower dark current density compared to the previously published AlGaN-based solar-blind *p-i-n* photodetector results in the literature.

The AlGaN *p-i-n* structure that was used in the present study was grown on double-side polished *c*-plane sapphire (Al_2O_3) substrates by low-pressure metal-organic chemical vapor deposition (MOCVD) system, which is located at the Bilkent University Nanotechnology Research Center. First, the wafer surface was cleaned by desorption in a H_2 environment at 1080 °C. Then, an ~100 Å AlN nucleation layer was grown at 550 °C by trimethylaluminum and ammonia (NH_3) under 50 mbar pressure. Subsequently, a high temperature (1135 °C) $Al_{0.4}Ga_{0.6}N$ buffer layer of 1600 Å was grown with trimethylgallium and a high flow NH_3 at 1160 °C. A N layer with a thickness of 5000 Å was grown with silane (SiH_4), in turn resulting in a carrier concentration of 10^{18} cm^{-3}. The growth continued with a 6000 Å $Al_{0.4}Ga_{0.6}N$ *i*-layer at 1130 °C. In the last step, a 1000 Å $Al_{0.4}Ga_{0.6}N$ *p*-layer with Mg doping by biscyclopentadienyl-magnesium was grown at 1050 °C. In all of the steps, the carrier gas was H_2 and the chamber pressure was kept at 50 mbar.

The samples were fabricated via a six-step microwave-compatible fabrication process in a class-100 clean room environment. The dry etching was accomplished by reactive ion etching (RIE) under CCl_2F_2 plasma, 20 SCCM (SCCM denotes cubic centimeter per minute at STP) gas flow rate, and 200 W rf power conditions. Mesa structures of the devices were formed via the RIE process by etching all of the layers (>1.2 μm) down to the nucleation layer for mesa isolation. After an Ohmic etch of ~0.7 μm, Ti:Al:Ti:Au (100 Å:1000 Å:100 Å:2000 Å) metal contacts and Ni:Au (100 Å:1000 Å) metal contacts were deposited by thermal evaporation and left in acetone for the lift-off process for N+ and P+ Ohmic contacts, respectively. The Ohmic contacts were annealed at 750 °C for 60 s. Thereafter, a 240 nm thick SiO_2 was deposited via plasma enhanced chemical vapor deposition for passivation. Finally, an ~0.3 μm thick Ti/Au interconnect metal was deposited and lifted off in order to connect the *n*-type and *p*-type Ohmic contact layers to the coplanar waveguide transmission line pads (Fig. 1).

For the present study, spectral transmission, current-voltage (*I-V*), and QE measurements were performed. *I-V* characterization of the fabricated photodetectors was carried out by using a 4142B electrometer and Keithley 6517A high resistance electrometer with low noise triax cables. QE measurements were performed using a xenon arc lamp, monochromator, UV-enhanced fiber, and SRS lock-in amplifier.

Solar blindness is guaranteed by the cutoff wavelength, which is 276 nm [Fig. 1(a)]. The *I-V* measurement results in Fig. 2 show that the 5 V bias dark current of a 200 μm diameter photodetector was 5 fA. This current level corre-

[a]Electronic mail: tturgut@fen.bilkent.edu.tr.

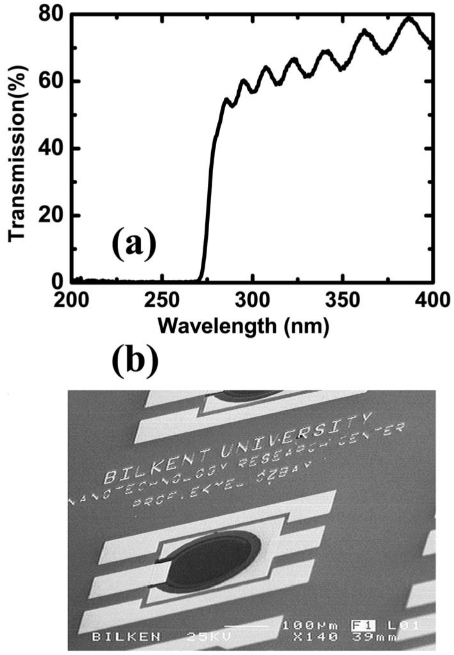

FIG. 1. (a) Spectral transmission of the wafer that was used in the fabrication of the detectors and (b) scanning electron microscopy image of 200 μm diameter fabricated devices.

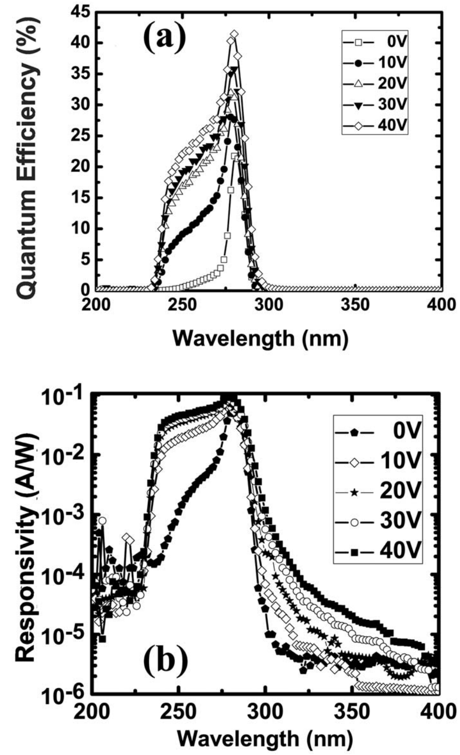

FIG. 3. (a) Spectral QE of the photodetector for varying reverse bias voltages and (b) responsivity of the photodetector for different reverse bias voltages.

sponds to the background noise floor of the electrometer that was used for the experiments, i.e., the minimum value that the electrometer can measure. The corresponding dark current density was 1.6×10^{-11} A/cm^2. The dark current at 120 V was 1.6 nA. The breakdown voltage of the photodetectors was measured as approximately 250 V. In terms of the breakdown voltage and dark current density at 5 V, these values correspond to the best results for AlGaN-based solar-blind *p*-*i*-*n*-type photodetectors.

A maximum 42% QE corresponding to 0.093 A/W responsivity at 280 nm under 40 V reverse bias and a 22% QE corresponding to 0.049 A/W under 0 V bias were achieved. The measured UV-visible rejection ratios of the photodetector were 1.64×10^4 and 1.22×10^4 for wavelengths larger than 375 nm under 0 and 40 V, respectively [Figs. 3(a) and 3(b)]. Neglecting the background radiation component, the thermally limited specific detectivity can be calculated with the thermally limited detectivity formula $D^*=R_\lambda(R_0A/4kT)^{1/2}$. In this formula, R_λ is the photovoltaic (zero bias) device responsivity, R_0 is the dark impedance at zero bias that is also known as differential resistance, and A is the detector area.[18,19] R_0 is found by fitting the dark current data with a curve fitting method as 1.25×10^{16} Ω.[20,21] Using the corresponding values for a 200 μm diameter device, thermally limited detectivity is calculated as $D^*=7.5\times10^{14}$ cm Hz$^{1/2}$/W which is a record value for AlGaN-based solar-blind *p*-*i*-*n* photodetectors reported in the literature.

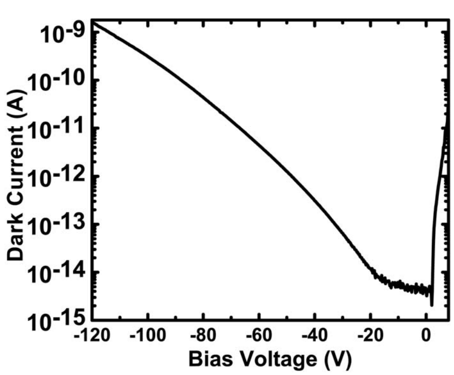

FIG. 2. Dark current of a 200 μm diameter AlGaN *p*-*i*-*n* photodetector.

In conclusion, we report the growth, fabrication, and characterization of high performance AlGaN-based *p*-*i*-*n* photodetectors. The optimized MOCVD growth conditions resulted in epitaxial samples that yielded high performance devices. A maximum 42% QE corresponding to 0.093 A/W responsivity at 280 nm under 40 V reverse bias and a 22% QE corresponding to 0.049 A/W under 0 V bias were achieved. The dark current of a 200 μm diameter circular diode was measured to be approximately 5 fA for voltages up to 10 V reverse bias, along with a breakdown voltage that was approximately 250 V. The solar-blind spectrum detectivity is calculated as $D^*=7.5\times10^{14}$ cm Hz$^{1/2}$/W at 280 nm. In terms of the breakdown voltage and detectivity, the reported results are better than the previously published AlGaN-based *p*-*i*-*n* photodetector results in the literature.

This work is supported by the European Union under the projects EU-NoE-METAMORPHOSE, EU-NoE-PHOREMOST, EU-PHOME, and EU-ECONAM, and TUBITAK under Project Nos. 105E066, 105A005, 106E198, 106A017, and 107A012. One of the authors (E.O.) also acknowledges partial support from the Turkish Academy of Sciences.

[1]M. Razeghi and A. Rogalski, J. Appl. Phys. **79**, 7433 (1996).
[2]E. Ozbay, N. Biyikli, I. Kimukin, T. Tut, T. Kartaloglu, and O. Aytur, IEEE J. Quantum Electron. **10**, 742 (2004).
[3]S. J. Pearton, J. C. Zolper, R. J. Shul, and F. Ren, J. Appl. Phys. **86**, 1 (1999).
[4]J. C. Campbell, S. Demiguel, F. Ma, A. Beck, X. Guo, S. Wang, X. Zheng,

X. Li, J. D. Beck, M. A. Kinch, A. Huntington, L. A. Coldren, J. Decobert, and N. Tscherptner, IEEE J. Quantum Electron. **10**, 777 (2004).
[5] M. Akazawa and H. Hasegawa, Phys. Status Solidi C **4**, 2629 (2007).
[6] J. B. Limb, D. Yoo, J. H. Ryou, W. Lee, S. C. Shen, R. D. Dupuis, M. L. Reed, C. J. Collins, M. Wraback, D. Hanser, E. Preble, N. M. Williams, and K. Evans, Appl. Phys. Lett. **89**, 011112 (2006).
[7] B. Yang, T. Li, K. Heng, C. Collins, S. Wang, J. C. Carrano, R. D. Dupuis, J. C. Campbell, M. J. Schurman, and I. T. Ferguson, IEEE J. Quantum Electron. **36**, 1389 (2000).
[8] K. A. McIntosh, R. J. Molnar, L. J. Mahoney, K. M. Molvar, N. Efremov, and S. Verghese, Appl. Phys. Lett. **76**, 3938 (2000).
[9] Q. Chen, J. W. Yang, A. Osinsky, S. Gangopadhyay, B. Lim, M. Z. Anwar, and M. Asif Khan, D. Kuksenkov, and H. Temkin, Appl. Phys. Lett. **70**, 2277 (1997).
[10] W. Yang, T. Nohova, S. Krishnankutty, R. Torreano, S. McPherson, and H. Marsh, Appl. Phys. Lett. **73**, 1086 (1998).
[11] J. C. Carrano, T. Li, D. L. Brown, P. A. Grudowski, C. J. Eiting, R. D. Dupuis, and J. C. Campbell, Appl. Phys. Lett. **73**, 2405 (1998).
[12] N. Biyikli, T. Kartaloglu, O. Aytur, I. Kimukin, and E. Ozbay, Appl. Phys. Lett. **79**, 2838 (2001).
[13] J. C. Carrano, T. Li, D. L. Brown, P. A. Grudowski, C. J. Eiting, R. D. Dupuis, and J. C. Campbell, Electron. Lett. **34**, 1779 (1998).
[14] R. McClintock, A. Yasan, K. Mayes, D. Shiell, S. R. Darvish, P. Kung, and M. Razeghi, Appl. Phys. Lett. **84**, 1248 (2004).
[15] R. McClintock, K. Mayes, A. Yasan, D. Shiell, P. Kung, and M. Razeghi, Appl. Phys. Lett. **86**, 011117 (2005).
[16] C. J. Collins, U. Chowdhury, M. M. Wong, B. Yang, A. L. Beck, R. D. Dupuis, and J. C. Campbell, Electron. Lett. **38**, 824 (2002).
[17] N. Biyikli, I. Kimukin, O. Aytur, and E. Ozbay, Electron. Lett. **16**, 1718 (2004).
[18] S. Donati, *Photodetectors: Devices, Circuits, and Applications* (Prentice-Hall, Englewood Cliffs, NJ, 2000).
[19] Ting Li, D. J. H. Lambert, M. M. Wong, C. J. Collins, B. Yang, A. L. Beck, U. Chowdhury, R. D. Dupuis, and J. C. Campbell, IEEE J. Quantum Electron. **37**, 538 (2001).
[20] N. Biyikli, O. Aytur, I. Kimukin, T. Tut, and E. Ozbay, Appl. Phys. Lett. **81**, 3272 (2002).
[21] C. J. Collins, T. Li, D. J. H. Lambert, M. M. Wong, R. D. Dupuis, and J. C. Campbell, Appl. Phys. Lett. **77**, 2810 (2000).